


# Toroidal dipole excitation in cylindrically arranged dogbone metallic inclusions

cambridge.org/mrf

V. P. Sarin<sup>1</sup> , P. V. Vinesh<sup>1,2</sup>, M. Manoj<sup>2</sup>, C. K. Aanandan<sup>2</sup>, P. Mohanan<sup>2</sup>  
and K. Vasudevan<sup>2</sup>

<sup>1</sup>Department of Electronics, Government College Chittur, Palakkad, Kerala, India and <sup>2</sup>Centre for Research in Electromagnetics and Antennas, Cochin University of Science and Technology, Kochi, Kerala, India

## Research Paper

**Cite this article:** Sarin VP, Vinesh PV, Manoj M, Aanandan CK, Mohanan P, Vasudevan K (2021). Toroidal dipole excitation in cylindrically arranged dogbone metallic inclusions. *International Journal of Microwave and Wireless Technologies* **13**, 1025–1030. <https://doi.org/10.1017/S1759078720001683>

Received: 26 July 2020

Revised: 2 December 2020

Accepted: 2 December 2020

First published online: 7 January 2021

### Key words:

Toroidal dipoles; Multipole scattering; Forward scattering

### Author for correspondence:

V. P. Sarin, E-mail: [sarincrema@gmail.com](mailto:sarincrema@gmail.com)

## Abstract

A significant excitation of toroidal moments in cylindrically arranged dogbone metallic inclusions is validated and presented in this paper. The antiparallel poloidal currents excited on the front and back faces of the proposed cylindrical dogbone inclusions create strong magnetic field confinement at the center generating intense toroidal moments on the structure. The significant excitation of toroidal dipole moment causes an improvement in the scattering cross-section from the resonant system. The resonant mechanism is analyzed using the multipole scattering theory, and we used the scattering measurement techniques to characterize the structure experimentally in the microwave regime.

## Introduction

Plane-wave scattering from metamaterials exhibiting toroidal dipole moments is a rapidly growing research area. Toroidal multipole moment is the higher-order multipole in the multipole scattering expansion. When the object size approaches the order of incident wavelength, then multipole theory shows the presence of toroidal moments. For sub-wavelength particles, only the first-order electric and magnetic dipole moments will be excited. Kerker and coworkers pointed out that when the electric and magnetic moments on these sub-wavelength inclusions are equal in magnitude and oscillating in phase, then forward scattering is observed [1, 2]. An out-of-phase oscillation reduces the scattering cross-section of the object [3]. The lack of natural magnetic materials remained a bottleneck until Pendry *et al.* demonstrated the first practical realization of artificial magnetism using the so-called split-ring resonator array [4]. The practical applications of such metamaterials are listed in various review reports [5].

Recently, toroidal dipole excitation in metamaterials has gained considerable interest due to their promising electromagnetic behaviors such as high near-field energy localization, high Q-factor, etc. Toroidal moments are created by the poloidal or the axial current distributions excited on the composite [6]. Classical electromagnetic theory neglects the excitation of this higher-order moment [7], and Zel'dovich first reported their excitation in nuclear systems [8]. Specially designed asymmetric configurations of split-ring resonators and stacked structures show toroidal moments [9–12]. Dielectric resonator-based techniques are also employed to overcome losses due to conduction currents [13]. Toroidal moments are created in the visible and ultraviolet range, using silicon-based dielectric materials [14, 15]. Recently, scattering from composite metamaterial structures is manipulated using toroidal dipole moments. Toroidal dipole excitation also ensures coherent forward scattering [16, 17]. The parallel excitation of overlapped toroidal and electric dipole moments is an anapole, and the resulting structure is invisible to a radar located at the far-field [18, 19]. Recently, toroidal metamaterial with tunable resonant behavior is observed in the THz range [20].

The specialty of dogbone metamaterials is that its dimensions are the order of the operation wavelength at resonance. Hence, toroidal dipole moments could be excited in specialized cylindrical configurations of dogbone structures. One such design is the cylindrically arranged dogbone elements around a metallic target [16] and is a modification of the authors' cylindrical cloaking structure [21]. The authors also detected a Fano-like resonance profile by exciting strong magnetic resonance to create an electromagnetic invisibility cloaking scheme in a separate spectral window devoid of toroidal excitation [22]. This paper proposes a modified dogbone-based cylindrical structure that shows a significant improvement in toroidal excitation. The authors have used full-wave electromagnetic simulations for optimization, and back-scattering from the design is measured using PNA E8362B network analyzer.

## The geometry of the structure

The unit-cell structure is a modification of our previous work [16], and the main difference is that it is devoid of the enclosed metallic cylindrical target, as shown in Fig. 1. All the

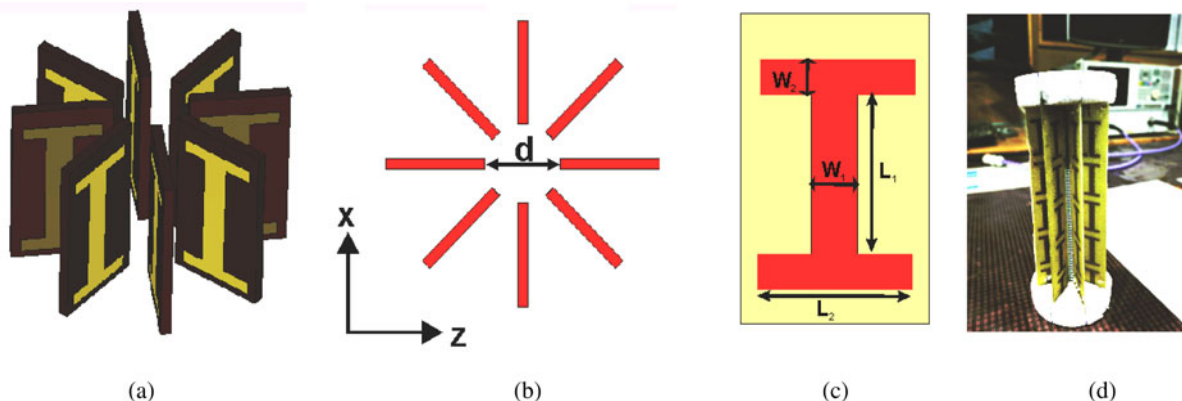


**Fig. 1.** Description of the structure under study. (a) Formation of the unit cell, (b) top view, (c) geometrical specifications ( $L_1 = 18$  mm,  $L_2 = 12$  mm,  $W_1 = 4$  mm,  $W_2 = 2$  mm,  $d = 14.5$  mm), and (d) photograph of the fabricated structure.

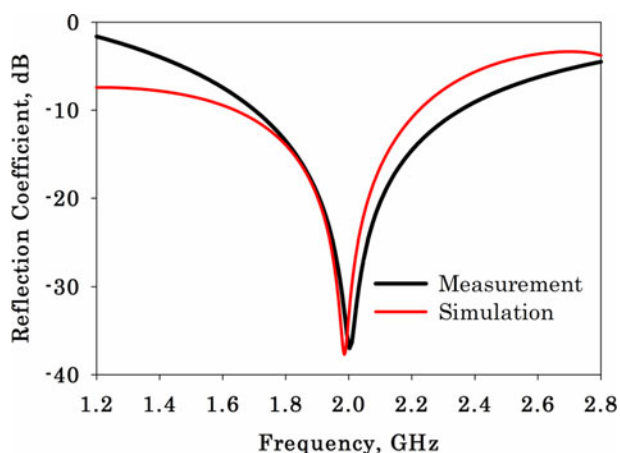


**Fig. 2.** Reflection coefficient of the proposed structure.

other parameters remain the same. Eight dogbone metallic elements, printed on a substrate of dielectric constant 4.4 and height 1.6 mm, are arranged in a coaxial fashion, as depicted in Fig. 1(a). Figure 1(b) shows the top view of the structure. The inner diameter  $d$  is selected to be 14.5 mm. Figure 1(c) illustrates the unit-cell dimensions. We have used photolithographic etching techniques for fabrication, and the engraved copper thickness is 35  $\mu\text{m}$ . The final full design used for measurement utilizes five such unit cells arranged vertically, as shown in Fig. 1(d).

### Simulation and measurement studies

We have used CST Microwave Studio for full-wave simulation studies of the structure. For that, a plane wave with polarization along  $y$ -axis is incident on the full structure shown in Fig. 1(d). Reflectance from the design is measured using a monostatic scattering measurement setup for normal incidence. For that, two ultra wideband antennas, with an azimuth offset of 5°, are mounted on a turntable assembly. We placed a metallic cylinder at the turntable assembly center for performing a THRU calibration. To avoid possible multipath clutters, proper time gating is

applied to receive reflections only from the target. Replacing the reference target with the studied structure gives the design's reflectance, as depicted in Fig. 2, and is well matched. The observed resonance is around 2 GHz, and it indicates strong back-scattering suppression at resonance.

The far-field scattering characteristics are studied using full-wave simulations and shown in Fig. 3. The scattering cross-section thus obtained for the structure compared with a metallic plane target is shown in Fig. 3(a). Around resonance, the design shows tremendous enhancement in scattered power as that of the bare metallic cylinder. Figures 3(b) and 3(c) compare the 3D scattering characteristics of both these structures. The cylindrical reference target shows omni-directional scattering, whereas the proposed structure scatters more power along the forward direction. Figures 3(d) and 3(e) represent the scattering patterns along the azimuth and elevation planes. It shows coherent forward scattering in both these planes. The 3 dB beamwidth is 57.6° and 111°, respectively, in these planes.

Multipole scattering theory helps to study the scattering contribution from different multipoles [9]. The power scattered from different multipoles is found by extracting the surface current distributions from the structure and then performing spatial integration as

$$P = \frac{1}{i\omega} \int J d^3r, \quad (1)$$

$$M = \frac{1}{2c} \int (\vec{r} \times J) d^3r, \quad (2)$$

$$T = \frac{1}{10c} \int [(\vec{r} \cdot J) - 2r^2 J] d^3r. \quad (3)$$

The results of these computations give scattered power from different multipoles. In the above equations,  $P$  and  $M$  represent the lower order electric, magnetic dipole moments,  $T$  represents the higher-order Toroidal dipole moment,  $c$  is the velocity of light in vacuum,  $\vec{r}$  is the displacement vector from the origin,  $\omega$  is the angular frequency, and  $J$  is the surface current density.

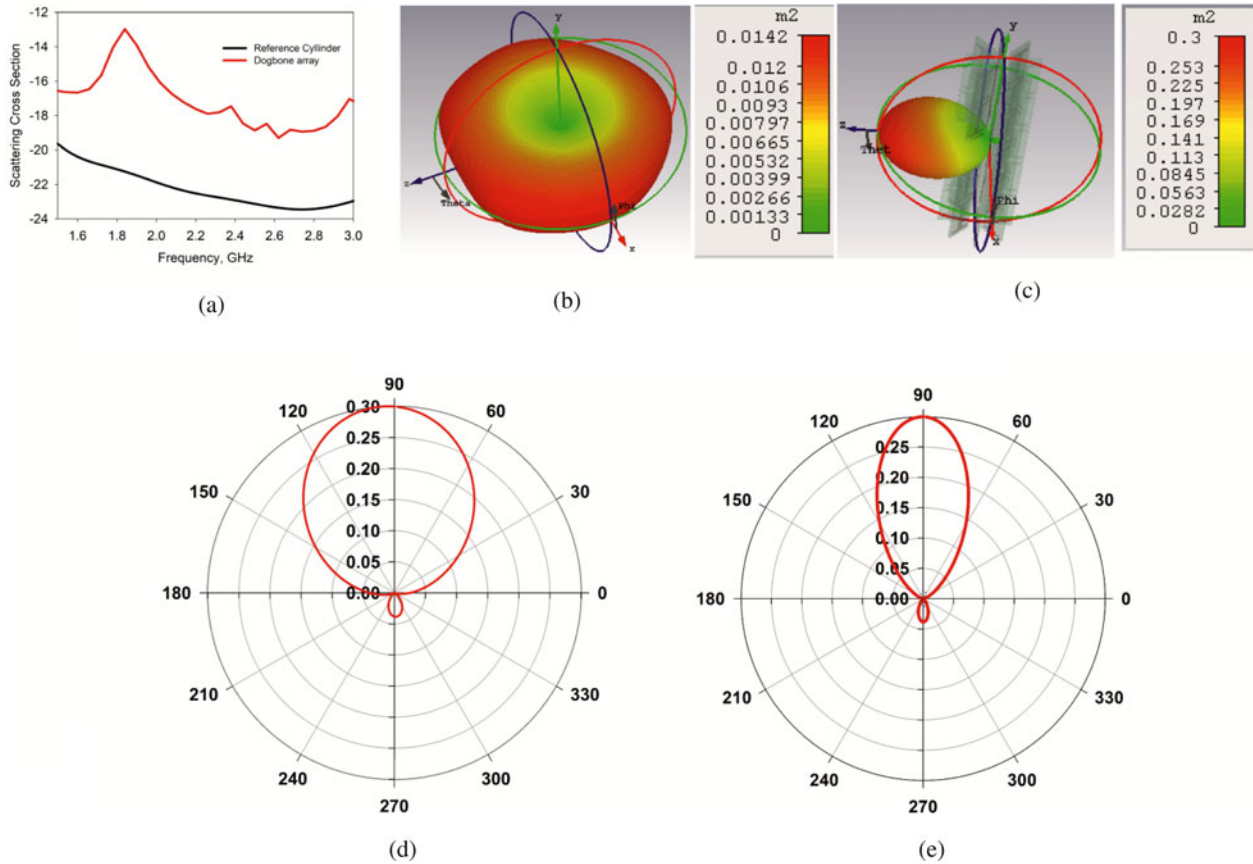


Fig. 3. Results of scattering studies performed. (a) Scattering cross-sections, (b) 3D scattering pattern of a bare metallic cylinder, (c) 3D scattering pattern of the proposed dogbone array, (d) azimuth plane RCS patterns, and (e) elevation plane RCS patterns.

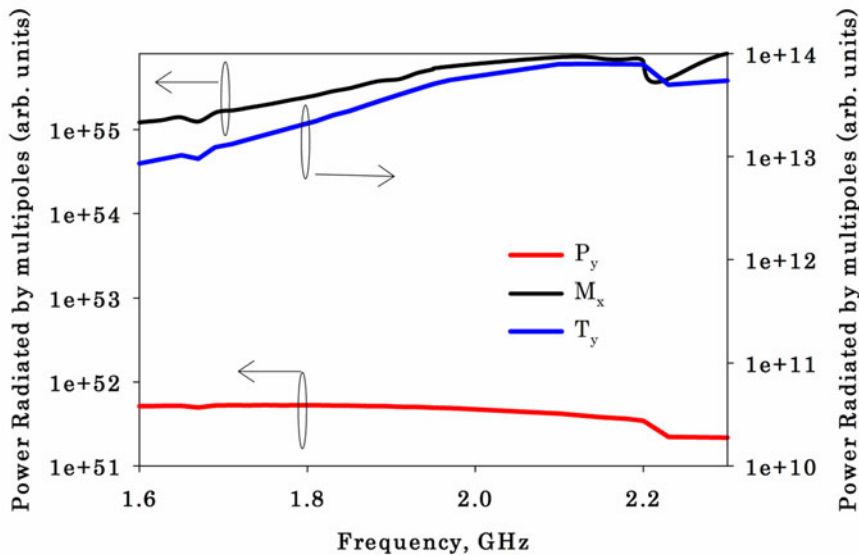
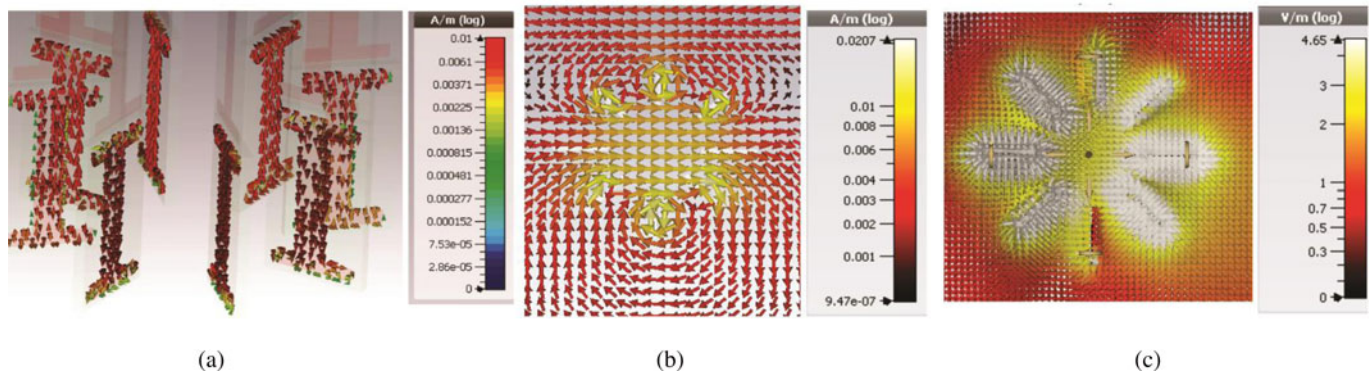
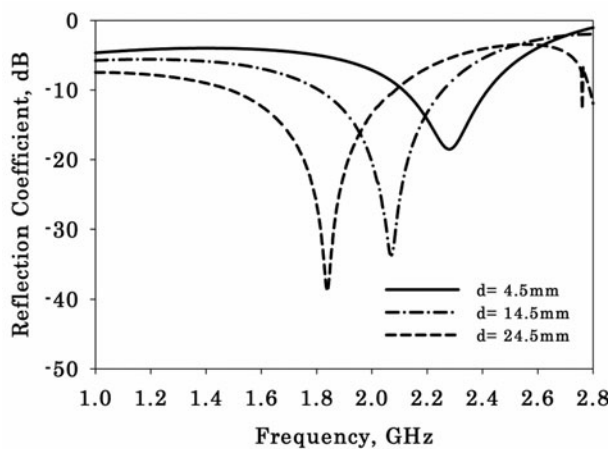


Fig. 4. Radiation contribution from different multipoles.



**Fig. 5.** Resonant field distributions on the structure. (a) Computed current distribution, (b) cross-sectional view of the magnetic field, and (c) electric field distributions.



**Fig. 6.** Effect of inner diameter on reflection coefficient for normal incidence.

Figure 4 illustrates the radiated power contribution from the  $P_y$  (electric),  $M_x$  (magnetic), and  $T_y$  (toroidal) moments. One could see here that power released from the magnetic dipole moment (black line) exceeds that from electric dipole moment  $P_y$  (red line) throughout the entire bandwidth under consideration. The power radiated from the magnetic moment  $M_x$  is 7000 times higher than that from the electric moment  $P_y$  at resonance. The radiated power contribution from the toroidal moment  $T_y$  is also indicated in the figure using a solid blue line. We could observe that power radiated from the toroidal moment is significantly high from this structure compared to our previous design [16]. The excitation of toroidal mode is responsible for coherent forward scattering from it at normal incidence.

The cross-sectional magnetic field distributions are useful in studying the excitation of toroidal moments on the structure. Figure 5 shows the resonant surface current and the cross-sectional magnetic fields excited on the cell. Figure 5(a) confirms that the surface currents excited on the structure's input entrance and output faces are out of phase. These antiparallel

current distributions create out-of-phase magnetic moments, creating strong in-phase magnetic field distribution at the center of the structure, causing toroidal moments  $T_y$ , as depicted in Fig. 5(b). The out-of-phase circulation of surface currents on the structure's input and output faces cancels the contribution of electric dipole moment  $P_y$  on far-field radiation. The unit-cell system will act as an efficient dielectric sensor because the enhanced magnetic energy density at the center of the structure enhances the sensor's sensitivity due to toroidal excitation. Figure 5(c) illustrates the computed cross-sectional electric field distribution at resonance. The electric field is concentrated on the top and bottom boundaries of the dogbone particle and is found minimum at the center where the magnetic field is maximum.

To study the effect of the inner diameter on reflection coefficient, we performed a detailed parametric analysis because this inner diameter significantly affects the coupling between dogbone metal strips. Figure 6 illustrates the effect of variation on reflection coefficient for normal incidence. An increase in the diameter of the cell redshifts the resonant frequency. The inner diameter increases the magnetic resonant patch length due to the significant increase in displacement current channel. Moreover, this change causes an increase in reflection from the structure, and the system becomes more inductive due to the enhancement in the mutual inductance between consecutive dogbone elements.

We performed the scattering measurements inside an anechoic chamber, and Fig. 7 illustrates these results. For that, the same methodology adopted for cloaking measurements is used [21]. Figure 7(a) shows the monostatic backscattered power from the structure for normal incidence. In this measurement, we rotated the design in the azimuth plane and recorded the received power. Measurements show that more than  $-20$  dB reduction in backscattered power is observed for all the azimuth angles at resonance. The polar plot of monostatic backscattered power at resonance shown in Fig. 7(b) verifies this observation. Figure 7(c) illustrates the measured bistatic radar cross section (RCS). A significant reduction in backscattered power better than  $-7.1$  dB is observed in comparison with the reference cylinder.

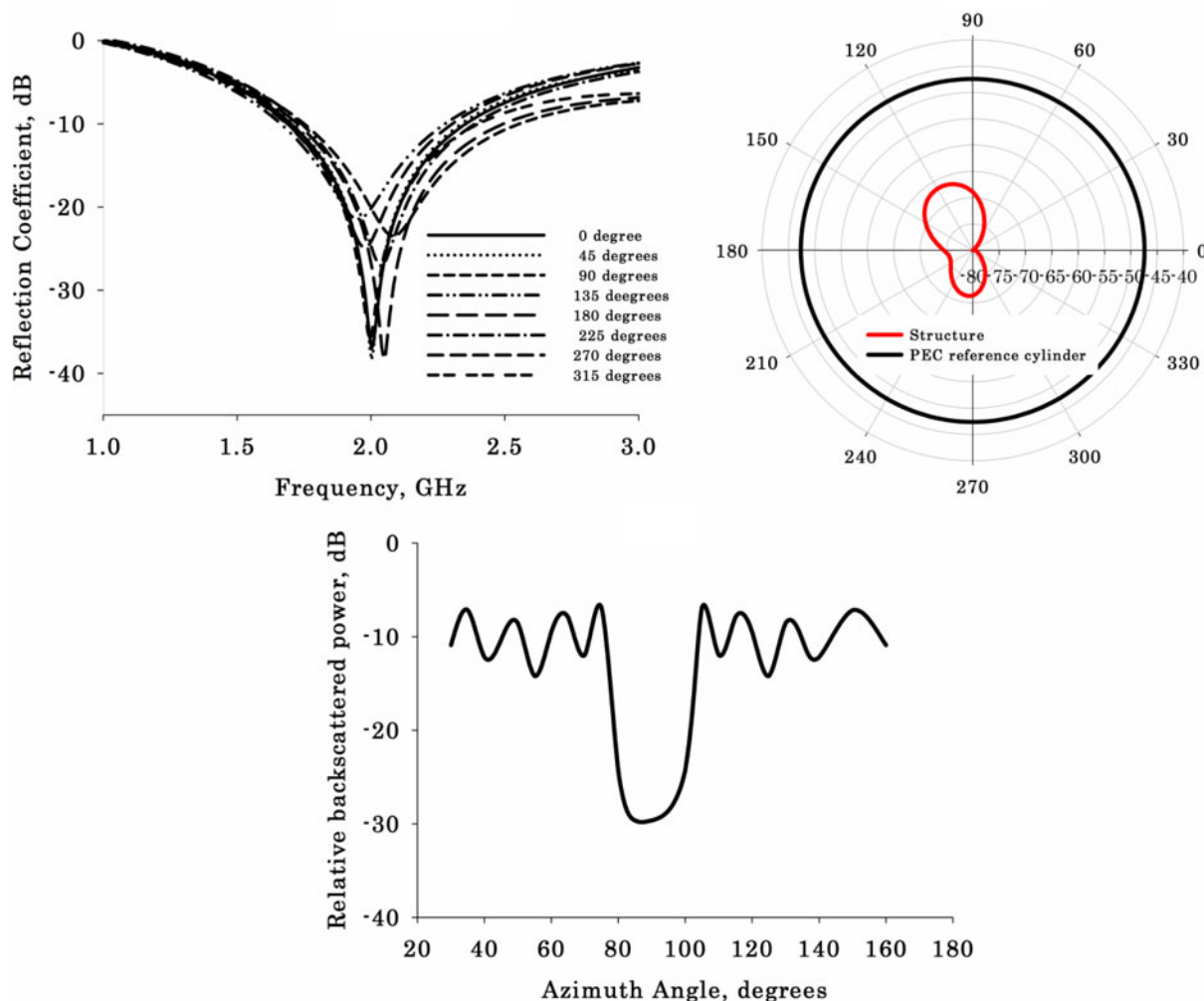


Fig. 7. Results of RCS measurements. (a) Monostatic measurements, (b) polar plot of monostatic backscattered power, and (c) bistatic measurements.

## Conclusions

This paper showed the physical excitation of toroidal moments on cylindrically arranged metallic dogbone inclusions in the microwave regime. The anti-phase magnetic moments excited on the structure's input and output faces create strongly enhanced magnetic field confinement at the center, yielding strongly enhanced toroidal moment. Multipole scattering reveals that significant excitation of magnetic and toroidal dipoles enhances forward scattering from the structure at resonance. The results are verified using full-wave electromagnetic simulations and are physically validated in experiments using radar cross-section measurements.

**Acknowledgements.** The research work is supported by the funding from the Science and Engineering Research Board (SERB), Department of Science and Technology (DST), Govt. of India for the major research project ECR/2017/002204.

## References

1. Kerker M, Wang DS, Chew H and Cooke DD (1980) Does Lorentz-Mie scattering theory for active particles leads to a paradox? *Applied Optics* **19**, 1231–1232.
2. Kerker M, Wang DS and Giles L (1983) Electromagnetic scattering by magnetic spheres. *Journal of the Optical Society of America* **73**, 765–767.
3. Kerker M (1975) Invisible bodies. *Journal of the Optical Society of America* **65**, 376–379.
4. Pendry JB, Holden AJ, Robbins DJ and Stewart WJ (1999) Magnetism from conductors and enhanced nonlinear phenomena. *IEEE Transactions on Microwave Theory and Techniques* **47**, 2075–2084.
5. Ziolkowski RW and Engheta N (2020) Metamaterials: two decades past and into their electromagnetics future and beyond. *IEEE Transactions on Antennas and Propagation* **63**, 1232–1237.
6. Afanasiev GN and Stepanovsky YP (1995) The electromagnetic field of elementary time-dependent toroidal sources. *Journal of Physics A: Mathematical and General* **28**, 4565.
7. Jackson JD (1999) *Classical Electrodynamics*, 3rd Edn. Hoboken: Wiley.
8. Zel'dovich IB (1958) The relation between decay asymmetry and dipole moment of elementary particles. *Journal of Experimental and Theoretical Physics* **6**, 1184.
9. Kaelberer T, Fedotov VA, Papasimakis N, Tsai DP and Zheludev NI (2010) Toroidal dipolar response in a metamaterial. *Science (New York, N.Y.)* **330**, 1510–1512.
10. Gupta M, Savinov V, Xu N, Cong L, Dayal G, Wang S, Zhang W, Zheludev NI and Singh R (2016) Sharp toroidal resonances in planar terahertz metasurfaces. *Advanced Materials* **28**, 8206–8211.
11. Gupta M and Singh R (2016) Toroidal versus Fano resonances in high Q planar THz metamaterials. *Advanced Optical Materials* **4**, 1–7; 201600553.
12. Fan Y, Wei Z, Li H, Chen H and Soukoulis CM (2013) Low-loss and high-Q planar metamaterial with toroidal moment. *Physical Review B* **87**, 115417.

13. Tazolamprou AC, Tsilipakos O, Kafesaki M, Soukoulis CM and Economou EN (2016) Toroidal eigenmodes in all-dielectric metamolecules. *Physical Review B* **94**, 205433.
14. Zografopoulos DC, Ferraro A, Algorri JF, Martín-Mateos P, García-Cámara B, Moreno-Oyervides A, Krozer V, Acedo P, Vergaz R, Sánchez-Pena JM and Beccherelli R (2019) All-dielectric silicon meta-surface with strong sub-tera hertz toroidal dipole resonance. *Advanced Optical Materials* **7**, 1900777.
15. Kuznetsov AI, Miroshnichenko AE, Brongersma ML, Kivshar YS and Luk'yanchuk B (2016) Optically resonant dielectric nanostructures. *Science (New York, N.Y.)* **354**, aag2472.
16. Sarin VP, Vinesh PV, Manoj M, Aanandan CK, Mohanan P and Vasudevan K (2020) Toroidal dipole-induced coherent forward scattering from a miniaturized cloaking structure. *Applied Physics A: Materials Science & Processing* **126**, 1–8.
17. Terekhov PD, Baryshnikova KV, Shalin AS, Karabchevsky A and Evlyukhin AB (2017) Toroidal dipole associated resonant forward scattering of light by Silicon nanoparticles. *Progress In Electromagnetics Research Symposium – Spring (PIERS)*.
18. Miroshnichenko AE, Evlyukhin AB, Yu YF, Bakker RM, Chipouline A, Kuznetsov AI, Luk'yanchuk B, Chichkov BN and Kivshar YS (2015) Nonradiating anapole modes in dielectric nanoparticles. *Nature Communications* **6**, 8069.
19. Nemkov NA, Stenishchev IV and Basharin AA (2017) Nontrivial non-radiating all-dielectric anapole. *Nature Scientific Reports* **7**, 1064.
20. Song Z, Deng Y, Zhou Y and Liu Z (2019) Terahertz toroidal metamaterial with tunable properties. *Optics Express* **27**, 5792–5797.
21. Sarin VP, Jayakrishnan MP, Vinesh PV, Aanandan CK, Mohanan P and Vasudevan K (2017) An experimental realization of cylindrical cloaking using dogbone metamaterials. *Canadian Journal of Physics* **95**, 927–932.
22. Pushpakaran SV, Vinesh PV, Manoj M, Aanandan C, Mohanan P and Kesavath V (2020) Demonstration of Fano resonance-based miniaturized cylindrical cloaking scheme. *Applied Physics A: Materials Science & Processing* **126**, 1–7.



**V. P. Sarin** received his M.Sc. degree in Applied Electronics in 2006 and the Ph.D. degree in Microwave Electronics from the Cochin University of Science and Technology, Kerala, India, in 2012. He is currently an Assistant Professor in the Department of Electronics, Government College Chittur, Palakkad, Kerala. His main research interests are metamaterials, microwave antennas, and FDTD techniques.



loop antennas, multiband antennas, etc.

**P. V. Vinesh** received the B.Sc. degree in Electronics from the University of Kannur, India, and the M.Sc. degree in Electronics from the MES College Erumely, Kottayam, India, in 2004 and 2006, respectively. He is currently working toward the Ph.D. degree at the Cochin University of Science and Technology (CUSAT), Cochin, India. His research interests include designing planar inverted F antennas,



research interests include electrically small antennas, RFID tags, and antennas for biomedical applications.

**M. Manoj** received his M.Sc. in Electronics from the Cochin University of Science and Technology, Kerala, India, in 2015 and currently pursuing Ph.D. at the Centre for Research in Electromagnetics and Antennas. He was awarded the Junior Research Fellowship by the University Grants Commission in 2014 and had been working at the Cochin University of Science and Technology since 2015. His current



International Centre for Theoretical Physics (ICTP). His research interests include microstrip antennas, radar cross-section studies, and frequency-selective surfaces.

**C. K. Aanandan** was born in India. He received the M.Sc. and Ph.D. degrees from the Cochin University of Science and Technology (CUSAT), Cochin, India, in 1981 and 1987, respectively. Currently, he is a Professor in the Department of Electronics, CUSAT. From 1997 to 1998, he worked at the Centro Studi Propagazione E Antenne, Consiglio Nazionale Delle Ricerche, Torino, Italy, under the TRIL program of the



microstrip antennas, dielectric resonator antennas, superconducting microwave antennas, reduction of radar cross-sections, and polarization agile antennas.

**P. Mohanan** was born in India. He received the Ph.D. degree in Microwave Antennas from the Cochin University of Science and Technology (CUSAT), Cochin, India, in 1985. Previously, he worked as an Engineer at the Antenna Research and Development Laboratory, Bharat Electronics, Ghaziabad, India. Currently, he is a Professor in the Department of Electronics, CUSAT. He has published more than 100 refer-



enced journal papers and numerous conference articles. He also holds several patents in the areas of antennas and material science. His research areas include microstrip antennas, dielectric resonator antennas, superconducting microwave antennas, reduction of radar cross-sections, and polarization agile antennas.

**K. Vasudevan** (SM'84) was born in India. He received the M.Sc. degree in Physics from Calicut University, Kerala, India, and the Ph.D. degree from Cochin University, Cochin, India, in 1976 and 1982, respectively. From 1980 to 1984, he worked at St. Alberts' College Ernakulam, Kerala, India. In 1985, he joined the Electronics Department of CUSAT, where he is currently the Emeritus Professor. His

research interests include microstrip antennas, leaky wave antennas, and radar cross-section studies. Dr. Vasudevan is a Fellow of the Institution of Electronics and Telecommunication Engineers (India).